

Research Article

In-situ synthesis of graphene on surface of copper powder by rotary CVD and its application in fabrication of reinforced Cu-matrix composites

Qiao Xiao^{1,2}, Xiaou Yi³, Bo Jiang^{1,2}, Zehua Qin^{1,2}, Jun Hu^{1,2}, Yong Jiang^{1,2}, Huiqun Liu^{1,2}, Bin Wang^{1,2} and Danqing Yi^{1,2*}¹School of Materials Science and Engineering, Central South University, Changsha, P.R. China²Key Laboratory of Nonferrous Metal Materials Sciences and Engineering, Ministry of Education, Central South University, Changsha, P.R. China³School of Materials Science and Engineering, University of Science and Technology Beijing, P.R. China

Abstract

A novel approach has been developed for fabricating graphene (Gr) reinforced Cu composites. First, graphene was synthesized *in-situ* on surface of micron-sized copper powder through rotary chemical vapor deposition (RCVD). Then, the composite powders were hot pressed into bulk Gr-Cu composite pieces in vacuum. During RCVD, methane flow rate controlled the number of layers in synthesized graphene. Analyses of Raman spectroscopy suggested that graphene with varied layer numbers were formed on Cu powder surface. The as-fabricated graphene exhibited a 'wrinkle' type morphology with a homogeneous distribution observed by field emission scanning electron microscopy (SEM). After hot pressing, the structure and morphology of graphene were preserved in the Gr-Cu bulk composites, as confirmed by high-resolution transmission electron microscopy (HRTEM). Physical and mechanical properties of these bulk composites were studied. They were nearly fully densified and featured with an increase of more than 30% in hardness, as well as similar electrical conductivity and thermal conductivity as compared with pure Cu. The mechanism therein was discussed.

Introduction

Graphene (Gr), a two-dimensional single layer of carbon atoms densely packed in a honeycomb lattice [1], has generated considerable interest in recent years, owing to its outstanding comprehensive performance such as high modulus, thermal conductivity and electrical conductivity [2]. Its applications have been demonstrated in various fields such as microelectronic devices, transparent and flexible electrodes, electronic/chemical sensors, catalysts, energy conversion/storage, as well as reinforcing fillers in composites.

Particularly, graphene has been widely introduced into many metal matrices in order to overcome the performance limits of conventional structural materials [3]. To take advantage of its promising properties, one must ensure a homogeneous distribution of graphene and a good interfacial bonding with the matrix [4]. However, these requirements are often difficult to meet due to agglomeration in graphene [5] and its poor wetting with metals [1]. In order to mitigate these problems, various fabrication techniques have been introduced, including liquid metallurgy [6], powder metallurgy [7-11], electrochemical deposition [12], molecular level mixing [13,14] and *in-situ* synthesis through chemical vapor deposition (CVD) [15]. Among these, powder metallurgy is one of the most popular methods due to its simplicity and convenience. Nevertheless, it does not naturally lead to good mixing and must be handled with great care to retain the integrity of graphene [16]. Recently, Chen and his coworkers [5] employed molecular-level mixing and spark plasma sintering to fabricate Gr-Cu composites. They reported that the copper matrix had been strengthened evidently by the addition of graphene. However, this method involved a complex pre-treatment of graphene using strong acid and base, which introduced many defects in material and degraded its initial properties.

Superior to other methods, the fabrication strategy based on *in-situ* synthesis of graphene on metal powders through CVD followed by hot consolidation is not only simple and low cost, and more importantly, easy to achieve the desired dispersion of graphene [17] and good interfacial bonding with metal matrices [18]. So far, most *in-situ* CVD work in literature has been reported for developing carbon nanotubes (CNTs) and carbon nanofibers (CNFs) reinforced metal matrix composites [17-21], very few were dealt with Gr-metal matrix bulk composites [15] despite of some for *in-situ* CVD synthesis of Gr-metal composite powders [22-25].

Owing to the excellent thermal and electrical conductivity of graphene and copper, it is nature to develop graphene reinforced Cu composites. Resorting to an effective fabrication method, one shall expect to achieve an excellent combination of high strength and high electrical/thermal conductivity as compare to pure copper. Great efforts have been made to fabricate such material [13], but unfortunately, all Gr-Cu composites fabricated by various methods have not yet realized the desired high electrical and thermal conductivity despite of a remarkable increase in strength. Poor interfacial bonding between

Correspondence to: Danqing Yi, School of Materials Science and Engineering, Central South University, Changsha, Hunan 410083, P.R. China, Tel: +86-731-88830263; Fax: +86-731-88836320; E-mail: yioffice@csu.edu.cn, danqing@csu.edu.cn

Key words: Graphene, Cu-matrix composites, *in-situ* synthesis, rotary chemical vapor deposition

Received: March 28, 2017; **Accepted:** April 26, 2017; **Published:** April 29, 2017

graphene and copper is the key issue, as indicated by many researchers [5,10]. So, it is still demanded to develop an effective fabrication method to achieve reliable interfacial bonding.

In the current study, we employed a novel process to produce high quality Gr-Cu bulk composites with improved interfacial bonding. This approach involved *in-situ* synthesis of Gr-Cu composite powders using rotary chemical vapor deposition (RCVD) and the fabrication of Gr-Cu bulk composites by vacuum hot pressing. The schematic of fabrication process is given in Figure 1. In the RCVD process, two kinds of Gr-Cu composite powders were fabricated with different flow rates of methane. The micron-sized copper powder was initially placed in a specially-designed, rotary quartz tube with a round belly in the middle, rather than on a stationary quartz boat, so that it could spread evenly and interact sufficiently with reaction gases. Compared to the stationary CVD, the RCVD could treat a larger amount of composite powders per batch, thereby improving the deposition efficiency. Besides that, graphene could be synthesized and deposited more homogeneously on surface of Cu powder, enabling a perfect mixing of them. After consolidation by vacuum hot pressing, both single layer graphene and multilayer graphene were deeply embedded in the Cu matrix. The hot-pressed Gr-Cu bulk composites were nearly fully densified, exhibited higher hardness and almost the same electrical and thermal conductivity of pure Cu [Figure 1].

Experimental

Pretreatment of Cu powder

Raw copper powder was spherical with an average particle size of 32 μm and a purity of 99.6wt.%. The powder was first ultrasonic cleaned in 3M acetic acid solution for 10 min, followed by 3~5 washes in distilled water. Then, ultrasonic cleaning was repeated in alcohol and isopropanol for 10 min, respectively. Finally, the powder was dried in vacuum. These procedures can effectively remove organic contaminants and oxides on powder surfaces (Figure S1 in supporting information), in favor of the uniform nucleation of graphene on copper.

Production of Gr-Cu composite powders

A rotary quartz-tube furnace was used for *in-situ* synthesis of graphene on surface of copper powder. The central isothermal zone spans over 200 mm, about 1/3 of the total length of the tube (Figure S2 in supporting information). Pre-treated Cu powder (~15 g) was placed in this region. Detailed procedure for the RCVD of graphene under ambient pressure is described as follows (Figure S3 in supporting information).

1. Fix the spinning speed of quartz tube to 18 r min^{-1} until the end of graphene growth. Purge the tube with Ar (600 sccm, standard-state cubic centimeter per minute) for 5 min to remove air and heat it to 800°C under a constant flow of 450 sccm Ar and 150 sccm H_2 .
2. Hold the tube temperature at 800°C for 30 min.
3. Raise the tube temperature to 1000°C. Introduce CH_4 into the reactor tube, at a flow rate of 1 sccm for batch one and 4 sccm for batch two. Maintain the flow rate ratio of H_2 to CH_4 at 30 and the total gas flow rate ($\text{Ar} + \text{H}_2 + \text{CH}_4$) at 600 sccm.
4. After 45 min, cut the flow of CH_4 and cool the furnace to room temperature in flowing Ar (450 sccm) and H_2 (150 sccm).

Fabrication of Gr-Cu bulk composites

Gr-Cu composite powders were ground in an agate mortar, heat treated at 500°C for 30 min and then consolidated into Φ 20 mm discs by hot pressing in vacuum (30 MPa, 900°C, 60 min). Control sample of pure Cu was also prepared under the same pressing process, using pre-treated Cu powder.

Characterization

The presence and quality of graphene in composite powders were validated and examined by Raman spectroscopy (HORIBA Lab RAM HR). Morphological observation of the Gr-Cu composite powders was carried out using field emission scanning electron microscopy (SEM, FEI Nova Nano 230). Optical microscopy (OM, LEICA MC 120 HD) and high-resolution transmission electron microscopy (HRTEM, Titan G²60-300) were employed to observe the microstructure of the hot-pressed Gr-Cu bulk composites. The concentration of carbon in bulk composites was examined by infrared absorption using carbon and sulfur determinators (LECO CS 600).

The density of composites was measured by the Archimedes' method. The relative density was calculated as the ratio of experimental bulk density and theoretical density. Vickers hardness (HV) testing was performed using a digital hardness tester (HVS-5) at a load of 10 N and a dwell time of 10 s. Electrical conductivity was tested on an eddy current conductivity meter (FQR-7501A). Thermal conductivity measurements were carried out on a laser-flash apparatus (NETZSCH LFA 457MiroFlash).

Results and discussion

Microstructure of Gr-Cu composite powders and bulk composites

Two batches of Gr-Cu composite powders were synthesized *in-situ* through RCVD, at the CH_4 flow rates of 1 and 4 sccm, respectively. They were specified as P_1 and P_2 . Analysis of Raman spectroscopy confirmed the presence and quality of graphene in these powders. The results are presented in Figure 2a and 2b. The main features in the Raman spectra of composite powders were labelled as peaks 'D', 'G' and '2D', in correspondence with Raman shifts at around 1360, 1583 and 2723 cm^{-1} , respectively. Peak D is associated with the vibrations of carbon atoms with dangling bonds for the in-plane termination of disordered graphite, and its intensity increases with the increase of defects [26]. Vibrations in all sp^2 -bonded carbon atoms in a 2D hexagonal lattice and the double resonance (DR) process give rise to peak G and peak 2D, respectively [27]. Here, as the CH_4 flow rate rising from 1 to 4 sccm, the intensity ratio of peak D to peak G, I_D/I_G , increased from 0.12 to 0.27, implying that structural defects were present in the synthesized graphene and that the number density of defects was proportional to the flow rate of CH_4 . According to literature [28], a significant change in the shape and intensity of peak 2D would be present when shifting from single-layer to multilayer graphene. In addition, the intensity ratio of peak G to peak 2D, I_G/I_{2D} , increases with the layer number. A I_G/I_{2D} value greater than 1 is indicative of more than one layer [29]. In Figure 2a, the I_G/I_{2D} ratios of P_1 and P_2 were calculated to be 1.56 and 1.96, respectively, suggesting that the lower the CH_4 flow rate, the fewer the number of layers. The full width at half maximum (FWHM) of peak 2D in P_1 and P_2 (Figure 2b) were measured to be 71.48 cm^{-1} and 61.87 cm^{-1} , separately. Combining these features with the high-intensity peak G, the weak peak D and the sharp and near-symmetric appearance of peak 2D, we were able to conclude that multilayer graphene have been

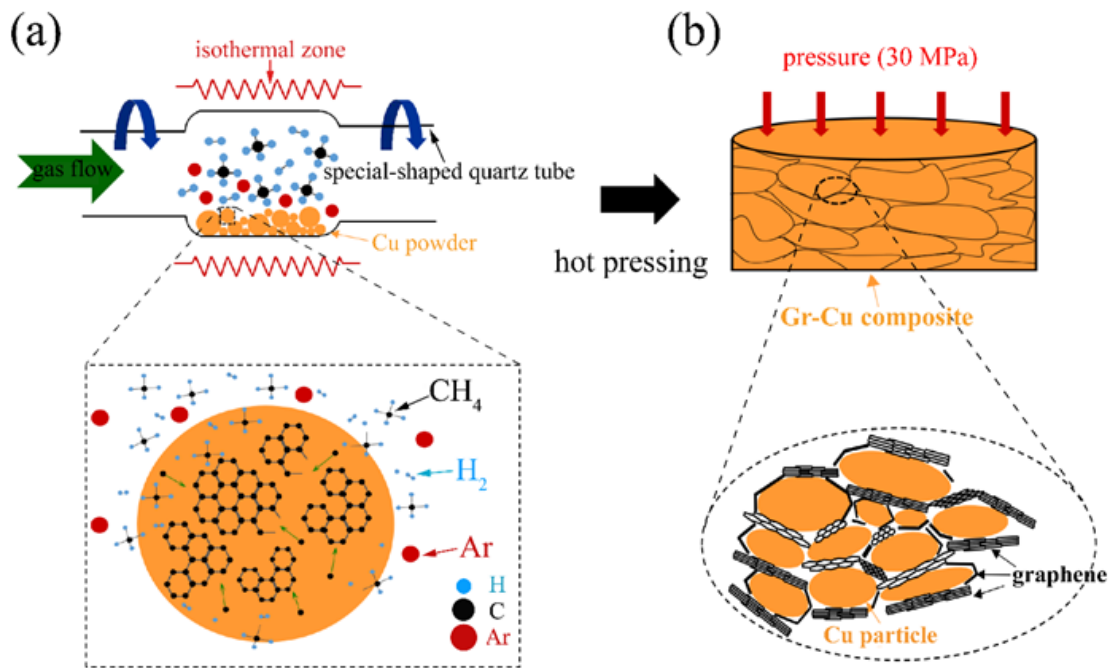


Figure 1. Schematic of fabrication process of Gr-Cu composites: (a) *in-situ* synthesis of Gr-Cu composite powders by RCVD, (b) fabrication of Gr-Cu bulk composites by vacuum hot pressing.

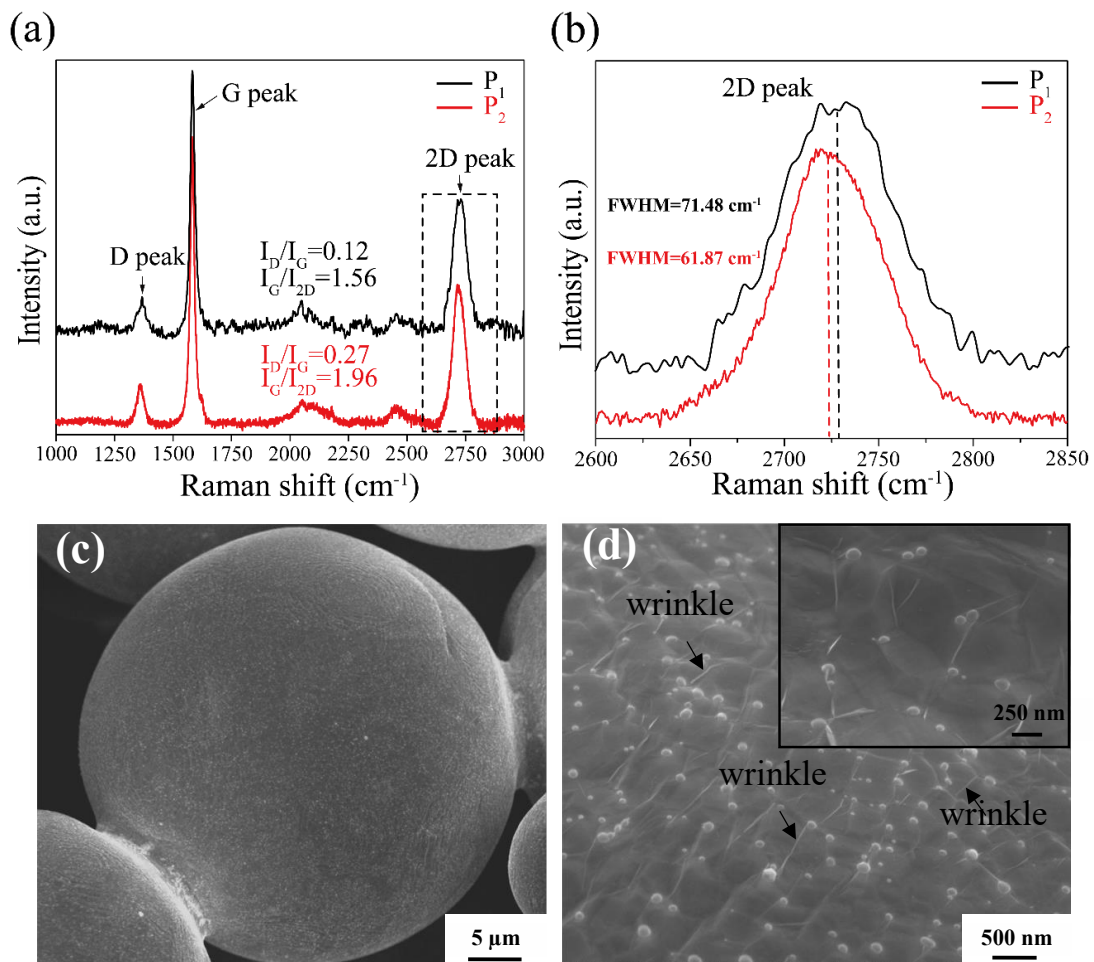


Figure 2. (a) Raman spectra and (b) peak 2D of P_1 and P_2 . (c) SEM image of an isolated particle of P_1 . (d) the high magnification image of the powder surface (inset image is higher magnification). (*In-situ* synthesized Gr-Cu composite powders produced by RCVD with 1 and 4 sccm CH_4 were designated as P_1 and P_2 , respectively.)

synthesized through RCVD, and the number of graphene layers and defect densities were tunable by the flow rate of CH_4 .

The SEM image of an isolated particle of P_1 is shown in Figure 2c. Under a higher magnification, the particle was covered by a net of ‘wrinkles’, as indicated by arrows in Figure 2d. These ‘wrinkles’ possibly formed during the cooling, owing to the difference in thermal expansion coefficients between Cu and graphene [30]. The uniform spread of the ‘wrinkles’ suggested that the distribution of graphene was rather homogeneous on surface of Cu powder. The inset image of Figure 2d reveals the detailed surface features of the P_1 particle. The high transparency of graphene net therein indicated that the *in-situ* synthesized graphene at the lower flow rate of CH_4 had only a few layers of atoms, being consistent with the Raman analysis in Figure 2a and 2b.

Gr-Cu bulk composites C_1 and C_2 were then fabricated from composite powders P_1 and P_2 by vacuum hot pressing. For a comparison, a control bulk sample of C_0 was also prepared using pre-treated copper powder. Microstructural characterization of these composites was carried out using TEM and HRTEM. Figure 3a shows the representative morphology of graphene exposed at the edge of ion-weakened pore in C_1 . Wrinkles and folds were easily visible on graphene surface with a large specific surface area and two-dimensional high aspect ratio sheet geometry. The ultrahigh transparency of graphene film indicated that it probably consisted of only a small number of atomic layers. Figure 3b is an HRTEM image of a graphene sheet. The presence of hexagonal patterns and non-regular hexagonal rings of carbon atoms were evident on the top of Cu lattice, indicating the successful preparation of single layer graphene sheet with some structural

defects. The graphene/copper interface structure is characterized in Figure 3c. Multilayer graphene was found to be curved, suggesting a good flexibility. The graphitic sheets in graphene were evident and the interlayer spacing among which was measured to be ~ 0.35 nm, very close to the ideal value of 0.34 nm, suggesting a good crystallinity. The lattice fringes of the matrix exhibiting an interlayer spacing of ~ 0.25 nm most likely represented the (110) planes of Cu. Combined with Figure 3b and 3c, one can conclude that both single-layer and well-crystallized multilayer graphene have been firmly embedded inside the Cu matrix, despite of the mechanical destruction during grinding and hot pressing. This shall be attributed to the high stability of *in-situ* synthesized graphene and its improved interfacial bonding with copper which were resulted from the RCVD and vacuum hot pressing. Nevertheless, amorphous carbon was also observed. This possibly gave rise to peak D in the Raman spectra in Figure 2a, and may account for why the electrical and thermal conductivity of composites were lower than one initially expected (Figure 4).

The performance of Gr-Cu bulk composites

The carbon content and the relative densities of hot-pressed pure Cu (C_0) and Gr-Cu bulk composites (C_1 and C_2) are summarized in Table 1. The carbon content of the composite can be tuned conveniently by adjusting the concentration of carbon source gas. As the flow rate of CH_4 increases, the carbon content in the composite increases accordingly. The relative densities of composites were found to be fairly high, ~ 99.0 and 99.6% , in contrast to 96.0% of pure Cu. This suggested that the *in-situ* synthesized graphene through RCVD was beneficial for the subsequent hot consolidation of Gr-Cu composite powders, and the latter possessed a good sintering ability [Table 1].

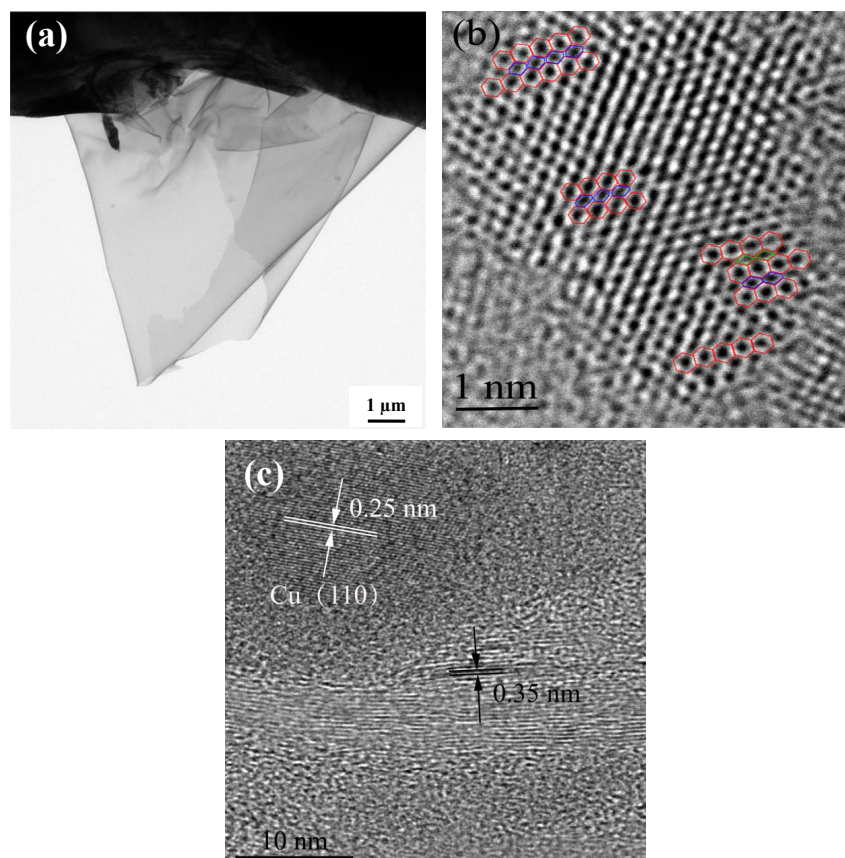


Figure 3. (a) TEM image of graphene exposed at the edge of ion-weakened pore in C_1 , (b) HRTEM image of graphene on surface of Cu in C_1 , (c) HRTEM image of C_1 . (the Gr-Cu bulk composite obtained from composite powder P_1 by vacuum hot pressing was specified as C_1 .)

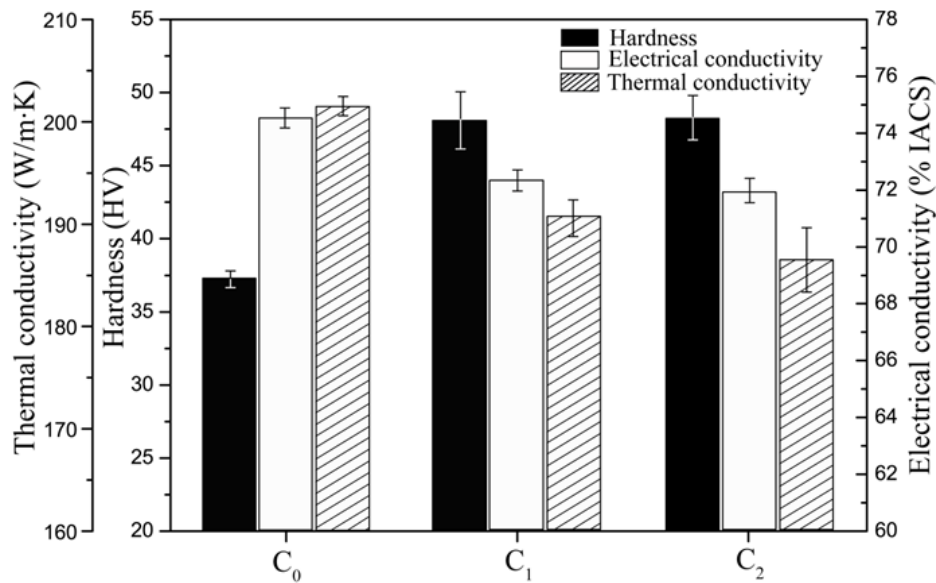


Figure 4. Measured hardness, electrical conductivity and thermal conductivity of C₀, C₁ and C₂ (C₀ was hot-pressed bulk pure Cu; C₁ and C₂ were hot-pressed 0.070 and 0.115 vol.% Gr-Cu bulk composites obtained from composite powders P₁ and P₂, respectively.)

Table 1. Carbon content and densities in hot-pressed pure Cu and Gr-Cu bulk composites.

Material	Carbon content [in wt.%]	Carbon content [in vol.%]	Theoretical density [g cm ⁻³]	Measured density [g cm ⁻³]	Relative density [%]
C ₀ ^{a)}	0	0	8.94	8.58	96.0
C ₁ ^{b)}	0.015	0.070	8.93	8.89	99.6
C ₂ ^{c)}	0.026	0.115	8.93	8.84	99.0

^{a)}hot-pressed pure Cu;

^{b)}hot-pressed 0.070 vol.% Gr-Cu bulk composite obtained from composite powder P₁;

^{c)}hot-pressed 0.115 vol.% Gr-Cu bulk composite obtained from composite powder P₂.

Hardness tests were further carried out to evaluate the mechanical performance of composites and the results are presented in Figure 4. The hardness of C₁ and C₂ was measured to be 48.19 and 48.43 HV, respectively, ~31.8 and 32.4% higher than that of C₀ (36.57 HV). The pronounced increase in hardness can be ascribed to the increase of graphene content.

The strengthening efficiency, R, that measures the strengthening effect of a given volume fraction of reinforcement on the matrix can be evaluated by Equation (1) [6]:

$$R = (H_c - H_m) / V_f H_m \quad (1)$$

where H_c and H_m are the hardness of composite and the matrix, respectively. V_f is the volume fraction of the reinforcement. In the present study, the strengthening efficiency R was calculated to be 454 and 282 for 0.070 and 0.115 vol.% graphene in C₁ and C₂, respectively. Note that this evaluation was rather rough and shall be regarded as the combined consequence of many important influences, such as interface bonding nature, relative density, and structural defect of graphene. For example, less structural defects indicate less loss of the intrinsic strength of graphene layers [14]. According to the above analysis, C₁ had a higher relative density than C₂ and the *in-situ* synthesized graphene therein had less structural defects. Consequently, the strengthening effect of graphene shall be more pronounced in C₁. Furthermore, it was worth noting that the strengthening efficiency of graphene in C₁ was remarkably higher than the literature data of Gr-Cu, Gr-Al, Gr-Mg bulk composites fabricated through other methods [5-7,9-11,14,31,32]. A summary of the comparison is given in Table S1

(supporting information). The remarkable strengthening achieved in this work shall be related to several factors as follows. Primarily, due to the use of RCVD, fine-sized copper powders were well wrapped by the *in-situ* synthesized graphene which can effectively impede grain growth and thus reduce the final grain size of Cu matrix as shown in Figure S4 (supporting information). The grain size refinement resulted in a high density of grain boundaries which effectively hindered dislocation movements [5]. In addition, graphene with ultra-high strength and homogeneous distribution in the Cu matrix may act as effective obstacle for preventing dislocation movements, therefore contributing to the strengthening of matrix [13]. Furthermore, the significant mismatch of thermal expansion coefficients (CTE) between graphene and copper matrix (in-plane CTE is $-6 \times 10^{-6} \text{K}^{-1}$ for graphene at 300 K and $24 \times 10^{-6} \text{K}^{-1}$ for Cu) may induce lattice distortion with a high dislocation density at the interface [14], further enhancing the strength. Finally, an increase in hardness was related to the improved interfacial bonding between Gr and Cu matrix (as suggested by TEM/HRTEM results in Figure 3). Compared with traditional fabrication methods such as powder metallurgy [7,9-11,31,32], carbonaceous nano-fillers were only mechanically mixed with metal powders prior to hot consolidation. Thus, the interfacial bonds with the metal matrix were not expected to be high [17], leading to a lower strengthening efficiency in the composites (Table S1 in supporting information).

The results of electrical and thermal conductivity measurements of hot-pressed pure Cu (C₀) and Gr-Cu bulk composites (C₁ and C₂) are compared in Figure 4. The conductivity values decreased slightly with increasing graphene content in the Gr-Cu composites. Specifically, the electrical and thermal conductivity values of C₂ were 72.02% IACS and 186.71 W m⁻¹K⁻¹, respectively, decreased by ~3.6 and 7.8% compared with C₀ (74.69% IACS and 202.46 W m⁻¹K⁻¹). The decrease in conductivity induced by graphene addition can be ascribed to the following reasons. First, the mean free path of electrons and heat carriers was reduced due to the reduction of grain size (Figure S4 in supporting information) [33].

Second, the interface between graphene and copper acted as a scattering center of electron transmission [10] and a thermal insulation barrier to heat flowing [5]. Third, the electrical and thermal conductivity

of graphene itself deteriorate significantly with increasing defects. Therefore, a poorer conductivity was found in the 0.115 vol.% Gr-Cu composite (C_2) which contained more defective graphene (Figure 2a). Nevertheless, the reduction in electrical/thermal conductivity caused by graphene addition was subtle. This shall be contributed to a very limited amount of porosity inside composites (Table 1 and Figure S4 in supporting information), an interlinked pathway of electrons and heat carriers induced by the well-dispersed graphene (Figure 2d) and the improved inter facial bonding between *in-situ* synthesized graphene and Cu matrix (Figure3).

Conclusions

In summary, Gr-Cu composite powders with multilayer graphene homogeneously dispersed on surface of Cu powder have been successfully prepared by RCVD. The Gr-Cu bulk composites with high quality interfacial bonding between graphene and Cu matrix were fabricated by hot pressing. They were nearly fully densified (ca. \cong 99.0% of theoretical density) and featured with an increase of more than 30% in hardness compared with pure Cu. High electrical conductivity (\cong 96.0% of pure Cu) and high thermal conductivity (\cong 92.0% of pure Cu) were also achieved.

It is worth mentioning that more work needs to be done to further improve the quality of graphene and its interfacial bonding with metal matrix by optimizing the RCVD parameters, such as the concentration of carbon source gas, the concentration ratio of hydrogen to carbon source gas and the spinning speed of quartz tube, and by replacing spherical metal powder with other-shaped (such as flaky) metal powder.

Acknowledgements

The authors gratefully acknowledge the National Natural Science Foundation of China (Grant No. 51474244) and the Shenzhen Science and Technology Project (Grant No. JCYJ20140509142357196) for providing financial support, and the Center for Analysis and Testing of Central South University for TEM and HRTEM characterizations.

References

- Moghadam AD, Omrani E, Menezes PL, Rohatgi PK (2015) Mechanical and tribological properties of self-lubricating metal matrix nanocomposites reinforced by carbon nanotubes (CNTs) and graphene-A review. *Compos Part B-Eng* 77: 402-420.
- Soldano C, Mahmood A, Dujardin E (2010) Production, properties and potential of graphene. *Carbon* 48: 2127-2150.
- Kumar HGP, Xavior MA (2014) Graphene reinforced metal matrix composite (GRMMC): a review. *Pro Eng* 97: 1033-1040.
- Neubauer E, Kitzmantel E, Hulman M, Angerer P (2010) Potential and challenges of metal-matrix-composites reinforced with carbon nanofibers and carbon nanotubes. *Compos Sci Technol* 70: 2228-2236.
- Chen F, Ying J, Wang Y, Du S, Liu Z, et al. (2016) Effects of graphene content on the microstructure and properties of copper matrix composites. *Carbon* 96: 836-842.
- Chen LY, Konishi H, Fehrenbacher A, Ma C, Xu JQ, et al. (2012) Novel nanoprocessing route for bulk graphene nanoplatelets reinforced metal matrix nanocomposites. *Scr Mater* 67: 29-32.
- Wang J, Li Z, Fan G, Pan H, Chen Z, et al. (2012) Reinforcement with graphene nanosheets in aluminum matrix composites. *Scr Mater* 66: 594-597.
- Tang Y, Yang X, Wang R, Li M (2014) Enhancement of the mechanical properties of graphene-copper composites with graphene-nickel hybrids. *Mater Sci Eng A* 599: 247-254.
- Rashad M, Pan F, Tang A, Asif M (2014) Effect of graphene nanoplatelets addition on mechanical properties of pure aluminum using a semi-powder method. *Prog Nat Sci-Mater* 24: 101-108.
- Jiang R, Zhou X, Fang Q, Liu Z (2016) Copper-graphene bulk composites with homogeneous graphene dispersion and enhanced mechanical properties. *Mater Sci Eng A* 654: 124-130.
- Li JL, Xiong YC, Wang XD, Yan SJ, Yang C, et al. (2015) Microstructure and tensile properties of bulk nanostructured aluminum/graphene composites prepared via cryomilling. *Mater Sci Eng A* 626: 400-405.
- Jagannadham K (2012) Electrical conductivity of copper-graphene composite films synthesized by electrochemical deposition with exfoliated graphene platelets. *J Vac Sci Technol B* 30: 03D109-1-9.
- Hwang J, Yoon T, Jin SH, Lee J, Kim T, et al. (2013) Enhanced mechanical properties of graphene/copper nanocomposites using a molecular-level mixing process. *Adv Mater* 25: 6724-6729.
- Zhang D, Zhan Z (2016) Strengthening effect of graphene derivatives in copper matrix composites. *J Alloy Compd* 654: 226-233.
- Nasibulin AG, Koltsova T, Nasibulina LI, Anoshkin IV, Semench A, et al. (2013) A novel approach to composite preparation by direct synthesis of carbon nanomaterial on matrix or filler particles. *Acta Mater* 61: 1862-1871.
- Tjong SC (2013) Recent progress in the development and properties of novel metal matrix nanocomposites reinforced with carbon nanotubes and graphene nanosheets. *Mater Sci Eng R* 74: 281-350.
- He C, Zhao N, Shi C, Du X, Li J, et al. (2007) An approach to obtaining homogeneously dispersed carbon nanotubes in Al powders for preparing reinforced Al-matrix composites. *Adv Mater* 19: 1128-1132.
- Kang J, Nash P, Li J, Shi C, Zhao N (2009) Achieving highly dispersed nanofibres at high loading in carbon nanofibre-metal composites. *Nanotechnology* 20: 235607. [Crossref]
- Yang X, Liu E, Shi C, He C, Li J, et al. (2013) Fabrication of carbon nanotube reinforced Al composites with well-balanced strength and ductility. *J Alloy Compd* 563: 216-220.
- Nasibulina LI, Koltsova TS, Joentakanen T, Nasibulin AG, Tolochko OV, et al. (2010) Direct synthesis of carbon nanofibers on the surface of copper powder. *Carbon* 48: 4559-4562.
- Kang J, Nash P, Li J, Shi C, Zhao N, et al. (2009) The effect of heat treatment on mechanical properties of carbon nanofiber reinforced copper matrix composites. *J Mater Sci* 44: 5602-5608.
- Li Y, Shi W, Chopra N (2016) Functionalization of multilayer carbon shell-encapsulated gold nanoparticles for surface-enhanced Raman scattering sensing and DNA immobilization. *Carbon* 100: 165-177.
- Liu Y, Hu Y, Zhang J (2014) Few-layer graphene-encapsulated metal nanoparticles for surface-enhanced Raman spectroscopy. *J Phys Chem C* 118: 8993-8998.
- Wang S, Huang X, He Y, Huang H, Wu Y, et al. (2012) Synthesis, growth mechanism and thermal stability of copper nanoparticles encapsulated by multi-layer graphene. *Carbon* 50: 2119-2125.
- Kang J, Li J, Shi C, Nash P, Chen D, et al. (2009) In situ synthesis of carbon onion/nanotube reinforcements in copper powders. *J Alloy Compd* 476: 869-873.
- Ferrari AC, Basko DM (2013) Raman spectroscopy as a versatile tool for studying the properties of graphene. *Nat Nanotechnol* 8: 235-246.
- Malard LM, Pimenta MA, Dresselhaus G, Dresselhaus MS (2009) Raman spectroscopy in graphene. *Phys Rep* 473: 51-87.
- Ferrari AC, Meyer JC, Scardaci V, Casiraghi C, Lazzeri M, et al. (2006) Raman spectrum of graphene and graphene layers. *Phys Rev Lett* 97: 187401. [Crossref]
- Robertson AW, Warner JH (2011) Hexagonal single crystal domains of few-layer graphene on copper foils. *Nano Lett* 11: 1182-1189. [Crossref]
- Wang Z, Liu Z, Monne MA, Wang S, Yu Q, et al. (2016) Interfacial separation and electrochemical delamination of CVD grown multilayer graphene for recyclable use of Cu powder. *RSC Adv* 6: 24865-24870.
- Li JF, Zhang L, Xiao JK, Zhou KC (2015) Sliding wear behavior of copper-based composites reinforced with graphene nanosheets and graphite. *Trans Nonferrous Met Soc China* 25: 3354-3362.
- Bartolucci SF, Paras J, Rafiee MA, Rafiee J, Lee S, et al. (2011) Graphene-aluminum nanocomposites. *Mater Sci Eng A* 528: 7933-7937.
- Goli P, Ning H, Li X, Lu CY, Novoselov KS, et al. (2014) Thermal properties of graphene-copper-graphene heterogeneous films. *Nano Lett* 14: 1497-1503. [Crossref]

Copyright: ©2017 Xiao Q. This is an open-access article distributed under the terms of the Creative Commons Attribution License, which permits unrestricted use, distribution, and reproduction in any medium, provided the original author and source are credited.